Statistics of extremal intensities for Gaussian interfaces

G. Györgyi,[1,*] P. C. W. Holdsworth,[2,†] B. Portelli,[2,‡] and Z. Rácz[1,2,§]
[1]*Institute for Theoretical Physics, HAS Research Group, Eötvös University, 1117 Budapest, Pázmány sétány 1/a, Hungary*
[2]*Laboratoire de Physique, Ecole Normale Supérieure, 46 Allée d'Italie, F-69364 Lyon cedex 07, France*
(Received 28 July 2003; published 21 November 2003)

The extremal Fourier intensities are studied for stationary Edwards-Wilkinson-type, Gaussian, interfaces with power-law dispersion. We calculate the probability distribution of the maximal intensity and find that, generically, it does not coincide with the distribution of the integrated power spectrum (i.e., roughness of the surface), nor does it obey any of the known extreme statistics limit distributions. The Fisher-Tippett-Gumbel limit distribution is, however, recovered in three cases: (i) in the nondispersive (white noise) limit, (ii) for high dimensions, and (iii) when only short-wavelength modes are kept. In the last two cases the limit distribution emerges in nonconventional scenarios.

DOI: 10.1103/PhysRevE.68.056116 PACS number(s): 05.70.−a, 05.40.−a, 68.35.Ct, 89.75.Da

I. INTRODUCTION

Extreme value statistics (EVS) has traditionally found applications in the analysis of environmental and engineering data, such as water level fluctuations or appliance lifetime [1]. Recently there has been a surge of activity from physicists in modeling phenomena that are governed by the extremal values of some random variable. Examples range from the low-temperature state in spin glasses [2], a variety of disordered systems with traveling fronts (see Ref. [3] for a brief review), and modeling corrosive fracture [4], to depinning of surfaces [5,6], to relaxation in granular materials [7].

A central notion in EVS is the existence of limit distributions, that is, the extremal value in a batch of a large number of independent, identically distributed (iid) random scalar variables obeys a probability density function (PDF), which is limited to one of three main types [1,8,9]. It is the tail of the PDF of the original variable, the parent PDF, that determines which one of these three classes the EVS will belong to. One distinguishes the Fisher-Tippett-Gumbel (FTG) distribution, for a decay faster than any power law, the Fisher-Tippett-Fréchet (FTF), for power tail, and Weibull, for power law at a finite edge. The limit PDFs can even be cast into a single function with a parameter whose different ranges correspond to different traditional classes, see, e.g., Ref. [1].

The appearance of EVS limit distributions in physical systems is in itself interesting and yields a new tool for the description of those systems, see, e.g., Ref. [2]. On the other hand, there are instances when the quantities in question are either dependent, differently distributed or have several components and thus generically do not belong to any of the aforementioned EVS classes, see, e.g., Refs. [5,10,11]. Closely related to our present subject are the studies on the distribution of local [12–14] and global [15] extrema of the height of surfaces. Whereas there is no general mathematical theory for the EVS of non-iid quantities, quite a few special cases have been clarified, Refs. [1,8] have some examples of them.

A possible connection of EVS to non-Gaussian fluctuations of spatially averaged, or, global, quantities in critical (strongly correlated) systems has recently been raised [5,16–21] in relation to both experiments [16,21–25] and simulations [26–28] for many-body systems as well as for environmental data [29,30]. There are two striking characteristics of this ensemble of observations. First, the form of the PDF is similar for these observables [16,26] and second, these functions bear a strong resemblance to the FTG distribution. There is some variation in form and there are some clear exceptions, but this approximate universality has been the subject of considerable debate in the literature.

More concrete connections to EVS have been found in studies of the fluctuations of the roughness, or width, of interfaces. The non-Gaussian nature of these fluctuations was first discussed in Ref. [31], and in Refs. [17,21,30,32–34] families of PDFs were identified, all characterized by a single maximum, positive skewness, an exponential, or near exponential, tail for large fluctuations above the mean, and even faster decay below it. In Gaussian interface models a relation to the FTG distribution has been observed in several instances. Namely, the magnetization distribution of the 2D (two-dimensional) XY model, in the low-temperature phase where vortices are rare, has been related to the roughness distribution in the stationary 2D Edwards-Wilkinson interface, and strong resemblance has been found to a formal generalization of the FTG function [26]. In another work on the 2D XY model, the FTG function was numerically observed for extremal mode selection [35]. A strong connection to EVS comes from an analytic result on a 1D interface model with long-range interactions, corresponding to a Gaussian noise with $1/f$ power spectrum, where the roughness of the interface turns out to be exactly of the FTG form [21].

Given the manifold occurrence of the FTG shape, we are led to study the relation between EVS and the roughness of Gaussian interface models. These models can be considered as generalizations of the stationary d-dimensional Edwards-Wilkinson interfaces, specified by the exponent α in the power-law dispersion of Fourier modes (for $\alpha=2$ the

*Electronic address: gyorgyi@glu.elte.hu
†Electronic address: pcwh@ens-lyon.fr
‡Electronic address: Baptiste.Portelli@ens-lyon.fr
§Electronic address: racz@poe.elte.hu

1063-651X/2003/68(5)/056116(14)/$20.00

Edwards-Wilkinson case is recovered). Due to their integrability, they are ideal starting point for the study of more complex, strongly fluctuating systems. As the models diagonalize into statistically independent modes, and the roughness equals the sum of the Fourier intensities, it is straightforward to address the problem of possible connection to EVS. Namely, one can pose the question that originally motivated our research: do the modes with the largest intensities dominate the PDF of the roughness? Here we show that the answer to this question is no. In fact, this negative result, the first main conclusion of this paper, is immediately apparent once we construct the distribution of the maximal intensity, an expression that turns out to be a generalized form of the Dedekind function. Besides being different from the distribution of roughness, this function generically also deviates from the FTG or any known EVS limit distributions. The reason for the deviation from conventional EVS is that the independent modes have gapless dispersion and are strongly nonidentically distributed even for higher wave numbers. As a result, for each realization of the interface, the largest intensity comes from one of only a few soft modes. The EVS is therefore effectively coming from a finite-size system, even in the thermodynamic limit.

The main body of the paper concerns the study of the maximal intensity PDF, which is found to depend on d and α. While there are no finite critical d_c or α_c, marking thresholds to the known EVS limit distributions, we discover three limits where FTG statistics sets in: (i) $\alpha\to 0$, (ii) $d\to\infty$, (iii) when only hard modes with wave vectors beyond a diverging radius R are kept. Common in these cases is that the thermodynamic limit can be taken beforehand, $N\to\infty$, where N is the total number of modes, so one chooses the maximal intensity out of an infinite set, in contrast to the conventional EVS procedure. The extremal value PDF becomes degenerate in all three cases in the sense that the standard deviation shrinks to zero on the scale of the mean. This is similar to the traditional FTG scenario when such degeneracy appears for $N\to\infty$. Now, however, in each case special scaling should be applied to resolve degeneracy and reveal the FTG distribution. It is suggested that the FTG limit in case (iii) is responsible for the numerically observed fit to the FTG function in Ref. [35].

Finally, we turn to the question how the EVS changes by considering a different choice of expansion functions (modes). This study further illuminates the fact that the EVS is not generically described by any of the traditional EVS limit functions. Since the dominant contribution to the EVS comes from a few modes, the EVS will depend on the specific expansion functions. We find analytically a different family of extreme value PDFs for the intensities if the interface is expanded in sines and cosines, albeit the overall shape goes close to that of the PDF of the maximal Fourier intensities.

We organize the paper as follows. In Sec. II we define the Gaussian model (Sec. II A), present the basic formulas for EVS for maximal Fourier intensities (Sec. II B), then in Sec. II C evaluate the EVS for the model showing $1/f$ noise. General $1/f^{\alpha}$ noise is considered in Sec. II D. The case of arbitrary substrate dimensionality is treated in Sec. III, with the general formulas for the extremal distributions calculated in Sec. III A. In Sec. III B the EVS for the magnetization modes for the XY system in the frame of the Gaussian model is investigated. The emergence of the FTG distribution in three limiting cases is described in Sec. IV. The EVS of square amplitudes from the expansion in sines and cosines is discussed in Sec. V. Section VI is devoted to a comparison to the distribution of the roughness, and Sec. VII contains the concluding remarks. The small-z asymptotes of the extremal value PDFs are derived in Appendixes A and B, and the finite-N correction to the extremal distribution is considered in Appendix C. Some details for the calculation of the PDF in the white noise limit is clarified in Appendix D, and in Appendix E we determine, for $\alpha>d$, the initial asymptote of the PDF of the roughness for comparison.

II. GAUSSIAN SURFACES IN ONE DIMENSION

A. $1/f^{\alpha}$ noise

The interface at position x on a one-dimensional $(d=1)$ substrate is characterized by the height $h(x)$. Replacing x by time t, $h(t)$ can be thought of as the distance from the origin of a random walker.

The roughness, or mean-square width, is given by

$$w_2(h)=\overline{[h(t)-\overline{h}]^2}, \tag{1}$$

where overbar denotes the average of walks, or interfaces in the interval $0\leq t\leq T$

$$\overline{F}=\frac{1}{T}\int_0^T F(t)dt. \tag{2}$$

The Fourier decomposition of the interface gives the amplitudes of the fluctuating modes we are interested in

$$h(t)=\sum_{n=-N}^{N} c_n e^{2\pi i n t/T}, \quad c_{-n}=c_n^{*}. \tag{3}$$

Here $h(t)$ is defined on N_0 equidistant points $(t=k\Delta t, T=N_0\Delta t)$ and we introduced the notation $N=(N_0-1)/2$, with N_0 assumed to be odd, before finally taking the thermodynamic limit $N\to\infty$. The roughness is then the integrated power spectrum

$$w_2(h)=\frac{1}{N}\sum_{n=1}^{N}|c_n|^2. \tag{4}$$

In the models we consider, the time signal $h(t)$ has periodic boundary condition, it exhibits $1/f^{\alpha}$ power spectrum, and the modes are independent Gaussian variables. The path probability is given by

$$\mathcal{P}[h(t)]\propto\exp\{-S[h(t)]\}, \tag{5}$$

where the action S is given in terms of Fourier intensities $|c_n|^2$ as

$$S=\sigma_0 T^{1-\alpha}\sum_{n=1}^{N} n^{\alpha}|c_n|^2, \tag{6}$$

with exponent α defining the $1/f^{\alpha}$ noise spectrum. σ_0 is a parameter setting the effective surface tension and the power of T originates from dimensional considerations [34].

The PDF of the roughness for the Gaussian model has been extensively studied in Refs. [20,21,34]. For $\alpha=1$ it was found analytically to coincide with the FTG function [21], one of the limit functions of EVS. Nevertheless, the roughness is not *a priori* an extremal quantity and it remains an open question why it obeys the EVS. One may argue that the sum is dominated by the softer modes whose extremal values possibly determine the cumulative behavior [18,35]. Motivated by this problem we study the largest contribution to sum (4).

An alternative choice of Fourier coefficients would be the set $(\mathrm{Re}\,c_n)^2,(\mathrm{Im}\,c_n)^2$, as studied in Ref. [35]. These are the coefficients from the expansions by sines and cosines, and while this does not seem to be a physically significant modification, the EVS for this set is, in general, quantitatively different from that of the intensities $|c_n|^2$. Nevertheless, the PDFs for the two sets are similar in shape and lead to the same physical conclusions, so we focus on the set $|c_n|^2$ along most of the main text, and summarize the results on the $(\mathrm{Re}c_n)^2,(\mathrm{Im}c_n)^2$ at the end.

B. Extreme value distributions

We calculate the probability that the maximal intensity $|c_n|^2_{\max}$ is $T^{\alpha-1}z/\sigma_0$, so we shall actually determine the scaling function of the EVS. We denote the PDF for that extreme value by $P_{\alpha}(z)$, and the cumulative or integrated probability distribution function (IPDF) by

$$M_{\alpha}(z)=\int_0^z P_{\alpha}(y)dy. \tag{7}$$

Since $M_{\alpha}(z)$ is the probability that none of $|c_n|^2$'s exceed $T^{\alpha-1}z/\sigma_0$, we can express it as

$$M_{\alpha}(z)=\prod_{n=1}^{N}\int_0^{|c_n|^2\leqslant z} A_n e^{-n^{\alpha}|c_n|^2} d\,\mathrm{Re}\,c_n\, d\,\mathrm{Im}\,c_n, \tag{8}$$

where $A_n=n^{\alpha}/\pi$ is the normalization constant for the PDF of the nth mode. After evaluating the integrals in Eq. (8) we find

$$M_{\alpha}(z)=\prod_{n=1}^{N}(1-e^{-n^{\alpha}z}). \tag{9}$$

In fact, for $\alpha=1$ product (9) is known from the defining formula of Dedekind's η function, the latter also containing an extra power prefactor [36]. Despite the difference in the prefactor, we will refer to Eq. (9) as a generalized Dedekind function. Differentiating (9) we arrive at the expression for the PDF of the maximal intensity

$$P_{\alpha}(z)=M_{\alpha}(z)\sum_{n=1}^{N}\frac{n^{\alpha}}{e^{n^{\alpha}z}-1}. \tag{10}$$

The IPDF and the PDF vanish for $z\leqslant 0$, the above formulas (9) and (10) are understood for non-negative z.

Three limits are easily understood here. First, if $\alpha=0$, i.e., the modes are identically distributed, we find

$$M_0(z)=(1-e^{-z})^N. \tag{11}$$

Then the change of variables $z=ay+\gamma+\ln N$, with

$$a=\sqrt{\zeta(2)}=\pi/\sqrt{6}, \tag{12a}$$

$$\gamma=\lim_{N\to\infty}\left(\sum_{n=1}^{N} n^{-1}-\ln N\right), \tag{12b}$$

where ζ is Riemann's zeta function and γ Euler's constant, yields the FTG distribution in the $N\to\infty$ limit

$$M_0(z(y))\to M_{\mathrm{FTG}}(y)=\exp[-e^{-ay-\gamma}], \tag{13a}$$

$$P_0(z(y))z'(y)\to P_{\mathrm{FTG}}(y)=a\exp[-ay-\gamma-e^{-ay-\gamma}]. \tag{13b}$$

The constants in Eq. (12) were used to scale the FTG distribution so that the mean becomes zero and the variance one [37]. Second and third, in both limits $\alpha\to\infty$ and $z\to\infty$ only the mode $n=1$ matters and one finds

$$M_{\alpha}(z\to\infty)\approx M_{\infty}(z)=1-e^{-z}, \tag{14a}$$

$$P_{\alpha}(z\to\infty)\approx P_{\infty}(z)=e^{-z}. \tag{14b}$$

Already at this point we can draw one of the main conclusions of the present paper, namely, that for general α the extreme value PDFs are none of the known EVS limit functions. This immediately follows from the fact that the negative-z and large-z behavior of Eqs. (9) and (10) is incompatible with those of the limit functions for the statistics of maxima [1,8].

The breakdown of validity of the traditional EVS limit distributions can be ascribed to the fact that, for $\alpha>0$, due to the n^{α} dispersion, the distributions of the individual modes are sufficiently different. Here "sufficiently" needs to be emphasized, because one can conceive sets of different parent PDFs for the modes [38] that lead to say the FTG function. Such is the case of a dispersion that has a gap at the origin or goes to a constant for high frequencies. Conversely, one should not be surprised by the appearance of special PDFs different from the known limit distributions, because actually for any given PDF one can choose sets of different parent distributions yielding that PDF in EVS [8].

It is easy to convince oneself that for $\alpha>0$ in formulas (9) and (10) the limit $N\to\infty$ can be taken and the resulting distribution has finite moments. Indeed, because of dispersion the exponential PDFs of individual modes decay increasingly fast and so no singularities appear for large N. In conventional EVS, limit distributions arise because the moments of variable z scale in singular ways in the thermody-

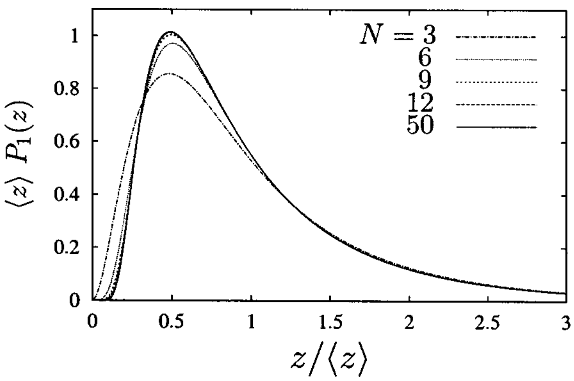

FIG. 1. Distribution functions for the $\alpha=1$ case evaluated numerically according to Eq. (10) for various N's, each function scaled to unit average. The convergence is apparently fast for practical purposes.

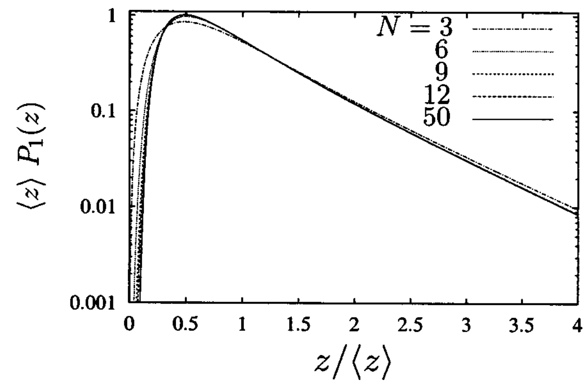

FIG. 2. The same as Fig. 1 on a semilogarithmic scale so as to better display the regions where $P_1(z)$ is small.

namic limit, thus removing most of the details of the distribution of the original random variables. Now, however, there is no such singular scale and the strong dependence on the statistics of the individual modes through the parameter α remains. This gives us a physical intuition about why the EVS for intensities of interfaces with dispersion is not described by any of the traditional limit distributions.

Furthermore, we can also immediately assert the difference between the PDF of the roughness (4), studied in Ref. [34], and PDF (10) of the maximal intensity component in Eq. (4). An obvious deviation is in the physical scales, namely, while the maximal intensity is always of order $T^{1-\alpha}$, the mean roughness is like that only for $\alpha>1$; it diverges logarithmically for $\alpha=1$, and stays finite for finite sampling times Δt if $\alpha<1$. Even when the scaling is the same, for finite $\alpha>1$, the two PDFs clearly differ [the generating function of the roughness PDF is given in Ref. [34], whose Laplace transform is not Eq. (10)], and become the same only in the limit $\alpha\rightarrow\infty$, when the $n=1$ mode dominates. A more detailed comparison will follow in Sec. VI.

C. 1/f noise ($\alpha=1$)

While for large z the PDF $P_1(z)$ is pure exponential as given in Eq. (14b), for general arguments one should resort to numerical evaluation. Function (10) is shown for a sequence of N's in Figs. 1 and 2. For $N\geqslant 9$ the curves are hard to distinguish by the naked eye, the approximation by finite N thus converges fast for practical purposes.

For small z, the expected nonanalytic behavior can be estimated in the following way: the product in Eq. (10) can be approximated as

$$M_1(z)\approx\prod_{n=1}^{1/z}(nz)\approx z^{1/z}\left(\frac{1}{z}\right)!\approx\sqrt{\frac{2\pi}{z}}e^{-1/z} \qquad (15)$$

where we have used Stirling's approximation for the factorial. While here we took the terms with $n>1/z$ as one, this gives us a first hint of the expected functional form. A more precise calculation in Appendix A shows that the large-n region gives a contribution of equal order, and in the end the true asymptote differs from Eq. (15) only in a scale factor in the exponent

$$M_1(z)\approx\sqrt{\frac{2\pi}{z}}e^{-\pi^2/6z}, \qquad (16)$$

see Eq. (A14) with Eq. (A12) for $\alpha=1$. Derivation by z gives the small-z asymptote of the PDF

$$P_1(z)\approx\frac{\sqrt{2\pi}\pi^2}{6z^{5/2}}e^{-\pi^2/6z}. \qquad (17)$$

As demonstrated in Fig. 3, the above expression is correct at small z and provides a reasonable approximation over most of the ascending part of $P_1(z)$.

We conclude the case of the $1/f$ noise by noting that the PDF for roughness (4) scales logarithmically in N and approaches the FTG function [21]. In contrast, as shown above, direct extremal selection of the constituent intensities in Eq. (4) leads to a nonsingular PDF, related to the Dedekind function, even in the thermodynamic limit. In short, we have the FTG distribution for the roughness, which is not an extremal quantity, while the EVS is not described by the FTG function. Thus the question raised in Ref. [21], namely, what kind of extremal value selection can possibly be responsible for

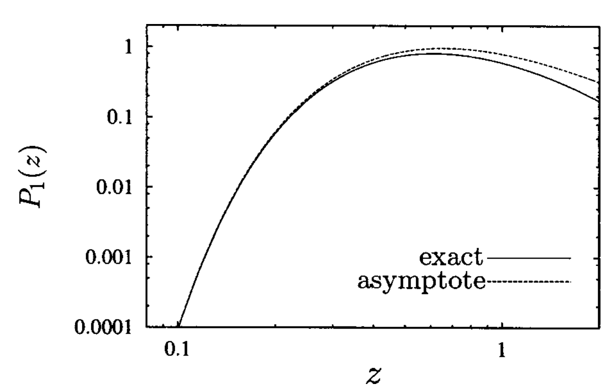

FIG. 3. The PDF $P_1(z)$ from Eq. (10) with $N=100$ and its small-z asymptote as given by Eq. (17).

the FTG distribution of the roughness, has not been answered and is left to further explorations.

D. General α

Here we go beyond the $1/f$ spectrum and investigate the noise for general α. The special cases $\alpha=0$ and $\alpha=2$ correspond to white noise and the Wiener process (ordinary random walk), respectively. The PDF of the roughness for Gaussian noise for periodic and "window" (bulk) boundary condition has been studied in Refs. [30,34], and no α other than 1 has been found for which the PDF coincided with any of the known limit PDFs of extreme statistics.

From the previous discussion it is clear that it is only for $\alpha=\alpha_c=0$ that EVS is given by the FTG function in finite dimensions. Concerning the small-z asymptote, the IPDF is given in Appendix A in Eq. (A14), whence differentiation yields the PDF

$$P_\alpha(z)\approx\frac{(2\pi)^{\alpha/2}c(\alpha)}{z^{3/2+1/\alpha}}\exp\left(-\frac{c(\alpha)}{z^{1/\alpha}}\right), \tag{18}$$

where $c(\alpha)$ is given in Eq. (A12). One can see that the above form becomes singular only in the $\alpha\to0$ limit. While for any finite $\alpha>0$ the asymptote is obviously incompatible with the FTG function (13b), surprisingly, expression (18) corresponds to the generalized FTF function for kth maximum [8] in the special case when k, the FTF power parameter μ, and α are related through $\mu=2(k-1)=1/\alpha$. Function (18) does not equal the EVS distribution for larger z, it is not even normalized to one, so this coincidence does not contradict the claim that the extreme value PDFs $P_\alpha(z)$ are none of the known limit distributions of EVS. The FTF class is not expected to be of relevance here anyhow because the parent PDFs of the constituent modes decay exponentially.

When one evaluates $P_\alpha(z)$, the convergence in N is important. The N dependence has been determined in Appendix C, whence it is apparent that convergence is fast for α of unit order and larger, but slows down for smaller α. We give here the asymptote in the region of slow decay, $\alpha<1$,

$$P_\alpha(z)-P_{N,\alpha}(z)\approx M_\alpha(z)\frac{N}{\alpha z}e^{-N^\alpha z}, \tag{19}$$

where we kept the N index for P when only N modes were counted.

The results of the evaluation of $P_\alpha(z)$ are given in Figs. 4 and 5. If displayed on the scale when the mean is set to one, see Fig. 4; for vanishing α the PDFs develop a singularity as eventually they approach the Dirac δ. Slow convergence in N for small α is also demonstrated; already for $\alpha=0.1$ one has to go up to exceedingly large N's to get a satisfactory approximation for the PDF. When the PDFs are shown with variance scaled to one, as in Fig. 5, the functions remain nonsingular and tend towards the FTG distribution.

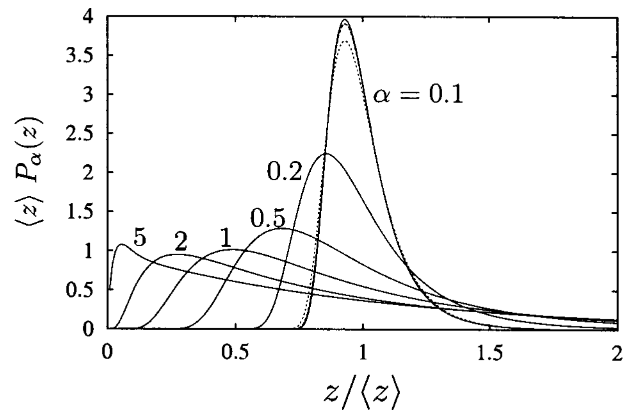

FIG. 4. Distribution functions for $d=1$ and various α's. We rescaled z by its mean $\langle z\rangle$ to get a variable of unit average. For $\alpha=0.1$ we show the sequence of approximants with $N=10^5,10^6,10^7$ peaks moving upwards with increasing N, to demonstrate slow convergence.

III. GENERAL DIMENSION

A. Extremal intensities

It is easy to generalize the above calculations to surfaces $h(\mathbf{r})$ defined on a hypercubic lattice substrate of dimension d and edge length L. We retain the periodic boundary condition for substrate, so the natural expansion of $h(\mathbf{r})$ involves again Fourier modes. The probability of a surface (5) is then characterized by the effective action [20,34]

$$S=\sigma_0L^{d-\alpha}\sum_{\boldsymbol{n}}^{N}{}' \ |\boldsymbol{n}|^\alpha|c_{\boldsymbol{n}}|^2. \tag{20}$$

Here the rescaled wave vector $\boldsymbol{n}=(n_1,n_2,\dots,n_d)$ has integer components n_i such that $|n_i|\leqslant N$, furthermore, the mark $'$ implies that if an $\boldsymbol{n}$ is counted then $-\boldsymbol{n}$ is not, and the zero vector is excluded. (The halving of the Brillouin zone is the consequence of the relation $c_{\boldsymbol{n}}=c^*_{-\boldsymbol{n}}$.) The above action for

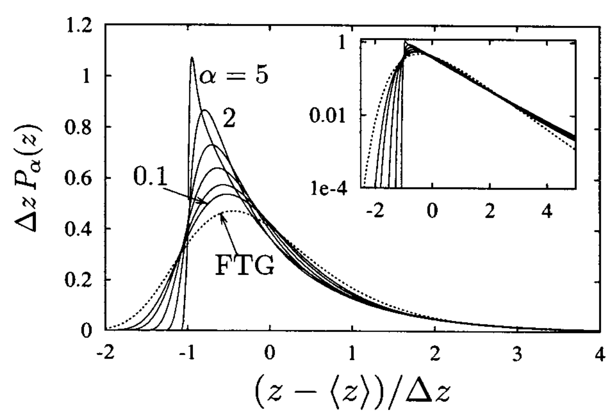

FIG. 5. The PDF with the same α's as in Fig. 4, but z is now shifted by its mean $\langle z\rangle$ and rescaled by its standard deviation Δz to produce a variable of zero average and unit deviation. For $\alpha=0.1$ only the curve with the largest N is shown. The peaks decrease with α. The PDFs tend to the FTG function (dashed line). The semilogarithmic inset magnifies the small-P regions.

$\alpha=2$ corresponds to the stationary state of the original Edwards-Wilkinson model, while for $\alpha=4$ it gives the curvature-driven Mullins-Herring interface. For a general $\alpha=2k$, k integer, it is a Gaussian massless model with finite-range, and for $\alpha\neq 2k$ with interactions decaying like a power law.

Denoting the maximal value of $\sigma_0 L^{d-\alpha}|c_{\boldsymbol{n}}|^2$ by z and its IPDF by $M_{\alpha,d}(z)$, each mode gives a multiplicative factor $1-e^{-|\boldsymbol{n}|^\alpha z}$ resulting in

$$M_{\alpha,d}(z)=\prod_{\boldsymbol{n}}^{N}{}' \left(1-e^{-|\boldsymbol{n}|^\alpha z}\right), \tag{21}$$

whence the PDF is

$$P_{\alpha,d}(z)=M_{\alpha,d}(z)\sum_{\boldsymbol{n}}^{N}{}' \frac{|\boldsymbol{n}|^\alpha}{e^{|\boldsymbol{n}|^\alpha z}-1}. \tag{22}$$

IPDF (21) can be considered as a further generalization of Dedekind's original product formula [36]. As in one dimension, it is straightforward to show that for $\alpha>0$ the above functions remain finite and involve finite mean and variance in the limit $N\to\infty$. Thus again no singular scaling is necessary and so we do not expect that any of the known extreme value limit PDFs emerge for general d and α. However, again as in $d=1$, for $\alpha=0$ all independent modes become identically distributed and we recover the FTG function after proper scaling by N.

The large α limit of Eq. (22), for any fixed dimension d, is determined by the contribution of the modes $|\boldsymbol{n}|=1$,

$$P_{\infty,d}(z)=d\,e^{-z}(1-e^{-z})^{d-1}. \tag{23}$$

For finite α where all modes count, we have closed forms only for the asymptotes. In the large-z limit, for any $\alpha>0$ and fixed d, one obtains

$$P_{\alpha,d}(z\to\infty)\approx d\,e^{-z}. \tag{24}$$

Since here, too, only the modes $|\boldsymbol{n}|=1$ matter, the large-z formula is obtained from PDF (23) for $\alpha\to\infty$, by taking $z\to\infty$, which explains the fact that Eq. (24) is independent of α. For $z\to 0$ we determined in Appendix A the asymptote of the logarithm of the IPDF $M_{\alpha,d}(z)$, see Eqs. (A15) and (A16). One can easily convince oneself that the leading term for the logarithm of $P_{\alpha,d}(z)$ is the same as for $M_{\alpha,d}(z)$, so we have for small z,

$$\ln P_{\alpha,d}(z)\approx-\frac{\pi^{d/2}\zeta\left(1+\dfrac{d}{\alpha}\right)\Gamma\left(1+\dfrac{d}{\alpha}\right)}{z^{d/\alpha}d\,\Gamma\left(\dfrac{d}{2}\right)}. \tag{25}$$

For general z we have to evaluate expression (22) numerically. This poses no difficulties unless $\alpha\approx 0$.

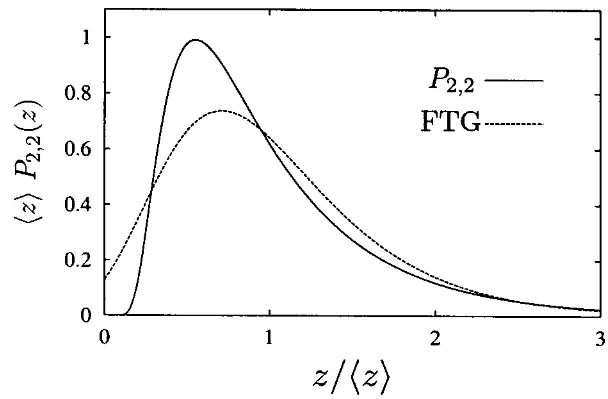

FIG. 6. Distribution function for the maximum Fourier intensity statistics for $d=\alpha=2$ and the FTG function scaled to unit mean and the same variance.

B. The 2D Edwards-Wilkinson model ($\alpha=2$)

One of the physically most relevant cases is $d=2$ and $\alpha=2$, the stationary Edwards-Wilkinson surface as originally defined. Since it is a massless Gaussian system, it also corresponds to the XY model in that part of the low-temperature phase where the effect of vortices is negligible [17]. There the magnetization distribution is proportional, with a change of sign, to the roughness of the Edwards-Wilkinson surface. Accordingly, the distribution of the maximum amplitude of the magnetization fluctuations, after proper scaling, should be given by PDF (22) for $d=\alpha=2$. Figure 6 shows $P_{2,2}(z)$ together with the FTG function normalized to the same mean and variance. While the fact that the two functions are different is obvious, here we demonstrate that the functions deviate significantly and in no range could they be mistaken for each other. The large difference here is of importance because the PDF $P_{2,2}(z)$ characterizes also the XY model, so this is an example when the FTG statistics is far from an EVS in a critical many-body system.

IV. FTG LIMITING CASES

A. Case (i): White noise limit $\alpha\to 0$

As we have seen, for $\alpha=0$ the modes become identically distributed in Eq. (21), thus, because of the exponential decay of the parent PDF for large z, one recovers the FTG function by proper scaling in N. One may, therefore, expect that when $N=\infty$ is set first, the extreme value distribution converges to FTG for $\alpha\to 0$, if proper scaling in α is applied. Such a convergence is not part of the standard theory of the FTG limit [1,8], so we show here how it comes about. A numerical demonstration in $d=1$ was given before in Fig. 5, now we derive it analytically for any d, and determine the natural scaling of the variable z by α.

Let us start out from the IPDF given by Eq. (21). Exponentiating the product into a sum, we realize that in the interesting region of z, where $-\ln M(z)$ is not too large, z must be large, thus we can linearize the logarithms. Then we notice that for small α the terms in the sum change slowly with $|\boldsymbol{n}|$, therefore we assume that the sum can be replaced by an integral. So we get

$$\ln M_{\alpha\to 0,d}(z) \approx -\frac{1}{2}\sum_{|\boldsymbol{n}|>0} e^{-|\boldsymbol{n}|^{\alpha} z}$$

$$\approx -\frac{\pi^{d/2}}{\Gamma(d/2)}\int_1^{\infty} e^{-n^{\alpha} z} n^{d-1} dn. \qquad (26)$$

Asymptotic analysis of this expression is done in Appendix D, and results in

$$\ln M_{\alpha\to 0,d}(z) \approx -A\left(\frac{\xi}{z}\right)^{d/\alpha}, \qquad (27)$$

where

$$\xi = \frac{d}{\alpha e}, \qquad (28a)$$

$$A = \frac{\pi^{d/2}}{\Gamma(d/2)}\sqrt{\frac{2\pi}{\alpha d}}, \qquad (28b)$$

valid in the region where z is ξ in leading order. Introducing the variable y by the linear transformation [for the constants a,γ see Eq. (12)]

$$z = \xi + \frac{1}{e}(ay + \gamma + \ln A), \qquad (29)$$

and keeping y of the order of unity when $\alpha \to 0$ we get

$$A\left(\frac{\xi}{z}\right)^{d/\alpha} \approx e^{-ay-\gamma}, \qquad (30)$$

up to terms vanishing with α. Since Eq. (27) was the leading term in the logarithm of the IPDF we get

$$M_{\alpha\to 0,d}(z) \approx e^{-e^{-ay-\gamma}}, \qquad (31)$$

which is IPDF (13a) for the FTG-distributed variable y. Since this IPDF has zero mean and unit variance, the linear transformation (29) is equivalently

$$z = \langle z\rangle + y\Delta z, \qquad (32)$$

where $\langle z\rangle$ is the mean and Δz the standard deviation of z up to terms vanishing for $\alpha \to 0$. It thus follows that the scaled maximal intensities z have an average diverging proportionally to α^{-1}, and they scatter in an $O(1)$ region about the average.

B. Case (ii): High dimensions

We immediately recognize the FTG limit when $d\to\infty$ in formula (23) of the PDF for large α, $P_{\infty,d}(z)$. Indeed, the PDF for the variable $y = (z-\gamma-\ln d)/a$ then goes over to the FTG limit function (13b). Below we study the $d\to\infty$ limit for any fixed positive α and conclude that again FTG arises. This is far from obvious *a priori* because while in large dimensions there are many modes in each shell of constant $|\boldsymbol{n}|$, so they have the same, exponential, parent distribution and, if we had only them, they would give rise to FTG, but on different shells the intensities are non-iid variables.

Again we exponentiate product (21) into a sum, and notice that if d is large, the entropic weight quickly increases with $|\boldsymbol{n}|$. Thus the dominant contribution comes from large $|\boldsymbol{n}|$'s, so we replace the sum by an integral and again get formula (26), which should be taken now for any fixed $\alpha > 0$ but in the limit $d\to\infty$. Its asymptotic analysis is similar to that described for $\alpha\to 0$ in Appendix D, and gives

$$\ln M_{\alpha,d\to\infty}(z) = -\frac{1}{\sqrt{2\alpha}}\left(\frac{\xi}{z}\right)^{d/\alpha}, \qquad (33)$$

where

$$\xi = \frac{(2\pi e)^{\alpha/2}}{\alpha e} d^{1-\alpha/2}, \qquad (34)$$

provided z is of the order of ξ. Next we introduce y through

$$z = \xi\left[1 + \frac{\alpha}{d}\left(ay + \gamma - \frac{\ln 2\alpha}{2}\right)\right]. \qquad (35)$$

Keeping y at order unity while $d\to\infty$, we get

$$\frac{1}{\sqrt{2\alpha}}\left(\frac{\xi}{z}\right)^{d/\alpha} \approx e^{-ay-\gamma}, \qquad (36)$$

whence Eq. (33) yields the IPDF

$$M_{\alpha,d\to\infty}(z) = e^{-e^{-ay-\gamma}}, \qquad (37)$$

which coincides with the FTG distribution (13a).

We can thus conclude that in high dimensions the extremal intensities belong to the FTG class. Furthermore, by comparing Eq. (32) with Eq. (35) we can determine the average and standard deviation of the scaled maximal intensity z, namely, $\langle z\rangle \propto d^{1-\alpha/2}$ and $\Delta z \propto d^{-\alpha/2}$. Interestingly, $\langle z\rangle$ diverges only for $\alpha<2$, while it shrinks to zero when $\alpha>2$, so the latter case is an example of a nonconventional FTG limit, when the maximal intensities are small although the intensities themselves are not bounded from above. While it is plausible that strong enough dispersion can have the effect of an upper cutoff on the amplitude, the novelty here is the sharp transition at $\alpha=2$, the only value when the characteristic maximal intensities remain finite and positive. For all $\alpha>0$, however, the scale of the standard deviation becomes much smaller than that of the average, a feature of the conventional FTG scenario [1,8].

C. Case (iii): Hard modes

We study the situation when the maximal amplitude is selected only from among those with $|\boldsymbol{n}| \geqslant R \gg 1$, that is, the very hard modes. We consider arbitrary but fixed α and d. Since we take the thermodynamic limit $N\to\infty$, we are left with a single divergent parameter R. Whereas all hard mode intensities are quite small, they are of different scales and so are essentially non-iid variables. Thus special considerations are necessary to determine their EVS.

The IPDF for the maximal hard mode amplitude is

$$M_{\alpha,d}(z,R)=\prod_{|\boldsymbol{n}|\geqslant R}{}^{\prime}\ (1-e^{-|\boldsymbol{n}|^{\alpha}z}). \tag{38}$$

Obviously $R=1$ gives the formerly studied IPDF (21) in the thermodynamic limit. The interesting region in z is where $M(z)$ changes fast. At this stage we assume that in that region $R^{\alpha}z$ is large, but we should check the result for consistency in the end. We can make from Eq. (38) a sum in the exponent, and since large $|\boldsymbol{n}|$'s are involved, we rewrite the sum into an integral. In leading order we obtain

$$\ln M_{\alpha,d}(z,R\to\infty)\approx-\frac{BR^{d-\alpha}}{z}\exp(-R^{\alpha}z), \tag{39}$$

where

$$B=\frac{\pi^{d/2}}{\alpha\,\Gamma(d/2)}. \tag{40}$$

Careful consideration of the compounding logarithmic singularities leads to the observation that in terms of the variable y, introduced by

$$z=R^{-\alpha}\left(ay+\gamma+\ln\frac{B}{d}+d\ln R-\ln\ln R\right), \tag{41}$$

expression (39) is just $-e^{-ay-\gamma}$ up to terms vanishing with increasing R. That is, we have recovered the FTG function (13a)

$$M_{\alpha,d}(z,R\to\infty)\approx e^{-e^{-ay-\gamma}}, \tag{42}$$

where the linear transformation (41) is understood. Comparing Eq. (41) with Eq. (32) we find that the mean $\langle z\rangle$ has the leading singularity $R^{-\alpha}\ln R$, so in the relevant region of z, $R^{\alpha}z$ indeed diverges, as assumed in the above derivation.

D. Scales of singularity

Summarizing the aforementioned limits, we found that FTG emerges (i) as $\alpha\to0$, (ii) for $d\to\infty$, and (iii) when only hard modes $R\leqslant|\boldsymbol{n}|$ with $R\to\infty$ are considered. While for $\alpha=0$ the intensities become iid and so FTG should be expected, they are *a priori* non-iid in the cases (ii) and (iii). Nevertheless, for $d\to\infty$ we found that a shell of practically iid modes in the Brillouin zone becomes dominant, so this essentially explains why one of the known EVS limit distributions emerged. On the other hand, in the case of hard modes we do not see iid intensities grouping, thus presently we lack an intuitive explanation for FTG. Remarkably, however, a common feature of all the above cases is that the distribution narrows down to a scale smaller than that of the average, a phenomenon also present in the traditional FTG scenario. In Table I we summarize the scales of the mean and standard deviation of the maximal amplitude, and compare them to the scales in the conventional limit when FTG

TABLE I. Order of the mean and standard deviation of the scaled maximal intensity z in the FTG limit cases (i)–(iii). For comparison the scales in the traditional scenario are also shown; see text for the parameters N,r.

Case	$\langle z\rangle$	$\Delta z=\sqrt{\langle z^2\rangle-\langle z\rangle^2}$	$\Delta z/\langle z\rangle$
(i) $\alpha\to0$	α^{-1}	1	α
(ii) $d\to\infty$	$d^{1-\alpha/2}$	$d^{-\alpha/2}$	d^{-1}
(iii) $R\to\infty$	$R^{-\alpha}\ln R$	$R^{-\alpha}$	$(\ln R)^{-1}$
iid $N\to\infty$	$(\ln N)^{1/r}$	$(\ln N)^{1/r-1}$	$(\ln N)^{-1}$

emerges. In the latter case we consider batches of iid variables, whose parent IPDF approaches 1 as $\exp(-az^r)$ for large z. The divergent parameter is then the number N of variables in a batch. Then the statistics of the maximal values within the batches becomes of FTG type [8], and straightforward calculation yields the scales given in the last row of the table.

V. SINE AND COSINE EXPANSION

Based on physical intuition one may suspect that, in the absence of the traditional EVS limit for iid variables, the extremal amplitude PDFs will depend on the choice of expansion functions. Given the periodic boundary conditions for the surface, another natural choice of expansion functions are the sines and cosines, whose coefficients squared are $(\mathrm{Re}\,c_{\boldsymbol{n}})^2,(\mathrm{Im}\,c_{\boldsymbol{n}})^2$. Below we show that indeed a new family of PDFs arise for the maximal square amplitude in this case, thus further illustrating deviation from the known EVS limit functions. More motivation to look at these coefficients comes from the fact that the first EVS study in this area was done with such an expansion in Ref. [35]. There, the FTG distribution was found numerically when soft modes were discarded.

When the sine and cosine modes are considered separately, we obtain the IPDF of $z\,L^{\alpha-d}/\sigma_0$ being the maximum of $\mathrm{Re}^2\,c_{\boldsymbol{n}}$ and $\mathrm{Im}^2\,c_{\boldsymbol{n}}$ as

$$\tilde{M}_{\alpha,d}(z)=\prod_{\boldsymbol{n}}^{N}{}^{\prime}\int_0^{\sqrt{z}}\int_0^{\sqrt{z}}A_n e^{-|\boldsymbol{n}|^{\alpha}|c_{\boldsymbol{n}}|^2}d\,\mathrm{Re}\,c_{\boldsymbol{n}}\,d\,\mathrm{Im}\,c_{\boldsymbol{n}}. \tag{43}$$

Then one straightforwardly gets

$$\tilde{M}_{\alpha,d}(z)=\prod_{\boldsymbol{n}}^{N}{}^{\prime}\ \mathrm{erf}^2(\sqrt{|\mathbf{n}|^{\alpha}z}), \tag{44}$$

whence

$$\tilde{P}_{\alpha,d}=\frac{2\tilde{M}_{\alpha,d}(z)}{\sqrt{\pi z}}\sum^{N}{}^{\prime}\ \frac{|\boldsymbol{n}|^{\alpha/2}e^{-|\boldsymbol{n}|^{\alpha}z}}{\mathrm{erf}(\sqrt{|\boldsymbol{n}|^{\alpha}z})}. \tag{45}$$

This will be the basis for numerical evaluation where we go up to an N where the curve in the figure visibly stabilizes.

For $\alpha\to\infty$ the $|\boldsymbol{n}|=1$ modes numbering $2d$ dominate, so

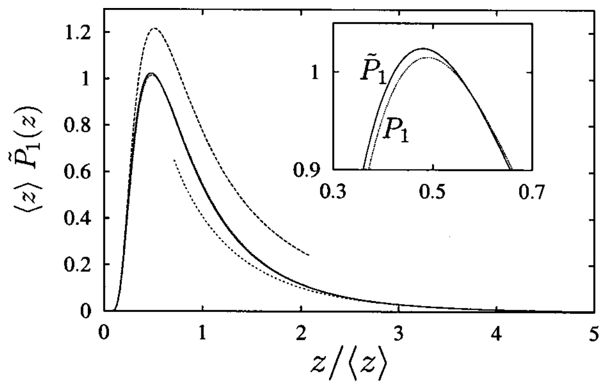

FIG. 7. The extreme value PDF $\tilde{P}_1(z)$, computed from Eq. (45) with $\alpha=d=1$ (full line), the asymptotes for small z from Eq. (47) (dashed), and for large z (48) (short dashed). For comparison the maximal intensity PDF $P_1(z)$ from Fig. 1 is also shown (dotted); the two PDFs are very close, but distinct, as can be observed also near the maximum (see inset).

$$\tilde{P}_{\infty,d}(z)=\frac{2de^{-z}}{\sqrt{\pi z}}\mathrm{erf}^{2d-1}(\sqrt{z}). \tag{46}$$

The large-z formula for any α is also determined by the softest modes, so it is just the asymptote of Eq. (46)

$$\tilde{P}_{\alpha,d}(z\to\infty)\approx\frac{2de^{-z}}{\sqrt{\pi z}}, \tag{47}$$

while for $z\to 0$ the logarithm of the PDF has the same leading term as the IPDF, given in Eqs. (B1) and (B2).

For the sake of demonstration we consider $\alpha=d=1$, and denote the corresponding PDF by $\tilde{P}_1$. For small z, Eq. (B3) of Appendix B with $\alpha=1$ gives the asymptote

$$\tilde{P}_1(z)\approx\frac{\pi c_1}{\sqrt{2}z^{5/2}}e^{-c_1/z}, \tag{48}$$

where $c_1=\tilde{c}(1,1)=1.332\,040\,5$ was computed from Eq. (B2). The full function and the asymptotic formulas are illustrated in Fig. 7. Note that the deviation of the small-z asymptote from the exact PDF never exceeds 0.25 even for larger z's. We also displayed the PDF of extremal intensity $P_1(z)$ from Fig. 1, which is given by a different formula and has a different mean $\langle z\rangle$, but after rescaling goes surprisingly close to $\tilde{P}_1$. Nevertheless, the two functions can still be distinguished as shown in the inset of Fig. 7. This demonstrates that in the present case the EVS depends weakly on the expansion functions.

Interestingly, in the three limits yielding the FTG distribution for the intensities $|c_i|^2$ in Sec. IV, the FTG function is found also for $(\mathrm{Re}\, c_{\boldsymbol{n}})^2,(\mathrm{Im}\, c_{\boldsymbol{n}})^2$, following derivations similar to the ones in Sec. IV C. So the FTG limits seem to be robust with respect to the choice of expansion functions. The FTG function found for the case of hard modes (the equivalent of the result in Sec. IV C) explains the finding of Ref. [35], where extremal square-coefficient statistics was studied numerically for the XY model, and the FTG function (13b) proved to be a good fit when soft modes were discarded from the batches of intensities before the selection of the maximal ones.

VI. COMPARISON WITH THE DISTRIBUTION OF THE ROUGHNESS

Interestingly, there is a resemblance between the scaling function of the extreme value PDFs for $\alpha>0$ and those for the roughness [34] for $\alpha>d$. Namely, both types of PDFs have a single maximum, positive skewness, a nonanalytic initial asymptote, and a dominantly exponential decay (the leading term in the logarithm of the PDF is linear for large z). However similar they are qualitatively, the functions are different.

A straightforward way to make the comparison quantitative is to calculate the asymptotes of the PDFs. For small x the roughness PDF behaves as given by Eq. (E16) of Appendix E, and the EVS PDF goes like Eq. (25). It is interesting to note that for the roughness the critical $\alpha_c=d$, where the variance shrinks to zero on the scale of the mean, while for the EVS the same type of criticality is observed for $\alpha_c=0$. Then both asymptotes can be cast in the common form

$$\ln P(y)\propto y^{-d/(\alpha-\alpha_c)}, \tag{49}$$

where for the roughness and for EVS one should understand y as z and x, respectively.

Furthermore, in 1D one can calculate the power prefactor in front of the nonanalytic exponential, cf. Eqs. (18) and (E9), that again can be written in the same form, so in 1D both PDFs are asymptotically

$$P(y)\approx C_1 y^{-[3(\alpha-\alpha_c)+2]/2(\alpha-\alpha_c)}\exp\left(-\frac{C_2}{y^{1/(\alpha-\alpha_c)}}\right), \tag{50}$$

albeit the proportionality constants in the two asymptotes are different. What is more, in 1D both PDFs become the FTG function in the limit $\alpha\to\alpha_c$. Note, however, that the two kinds of PDFs have different asymptotes for larger arguments, when $\alpha>\alpha_c$.

We can put the threshold behavior in a short form. First, for both kinds of distributions there is a (lower) critical value $(d/\alpha)_c^{\ell}$, where, for increasing d/α, on the scale of the mean the distributions become the Dirac δ, and this threshold is 1 for the roughness and ∞ for the EVS. Then there is an upper critical value $(d/\alpha)_c^u$, which is the threshold for the respective classical limit distribution, Gaussian for the roughness, and FTG for the maximal intensity. For the roughness we have seen [17,34] that $(d/\alpha)_c^u=2$ and for the maximal intensity it is again $(d/\alpha)_c^u=\infty$. So there is a region, $2\leqslant d/\alpha\leqslant\infty$, where the roughness is Gaussian, but the EVS is still not given by any of the known limit distributions of EVS, rather by the generalized Dedekind function.

There is a significant difference also in the finite-size correction to the PDF. The PDF for the extremal amplitude converges essentially exponentially fast (see Appendix C for the

1D correction formula), while the correction to the roughness PDF can be shown to be algebraic in N.

In sum, there is a strong qualitative resemblance between the shape of the roughness PDF for $\alpha > d$ and the EVS, furthermore, their initial asymptotes have similar functional forms, they are, however, distinctly different functions. It remains to be clarified whether the similarity has some deeper reason or it is simply a mathematical coincidence.

VII. CONCLUSION

The results presented above bring us to a very definite conclusion concerning the relation between interface fluctuations and extremal statistics: the roughness PDF is not given by the largest mode in the Gaussian interface model. This is true, even in the case $\alpha = d = 1$, where the roughness PDF is the FTG distribution [21], one of the known limit functions of extreme statistics. We showed, further, that the PDF was none of the known EVS limit distributions and depended on the statistics for the individual elements of the model. In addition, one expects the boundary conditions to influence the shape of the PDFs. It should be added that, to the extent that the Gaussian model is a universal family of massless models from the viewpoint of critical phenomena, the generalized Dedekind PDFs are equally universal, depending on the dimensionality d and the dispersion parameter α.

It is worth pointing out that there is an analogy between the Gaussian distribution arising from the central limit theorem, which applies for sums of random variables with finite moments, and the extreme value limit distributions such as FTG, which is about the maximal of those variables. Both limit distributions are related to a large ensemble of independent, identically distributed objects. The appearance of a non-Gaussian PDF for the integrated power spectrum (i.e., roughness), in Gaussian systems [16,17,21,23,26,31,32,34,35], is a consequence of strong dispersion, whence follows the strongly nonidentical distribution of the modes. What we have illustrated in this paper is that it is this same dispersion that generically excludes the known limit distributions of extreme statistics. To refine the picture, we found that if Gaussian central limit statistics is excluded for the integrated variable because of dispersion, FTG extremal statistics is also explicitly excluded, but the reverse is not necessarily true: there is the region of finite $d/\alpha \geqslant 2$, where the integrated power is Gaussian but the maximal Fourier intensity does not follow FTG. However, we found three border cases where, by singular scaling, the FTG distribution arises. In the limit $\alpha \to 0$ the amplitudes obviously become identically distributed. For the other cases, that is, in the limit $d \to \infty$ and when a large number of modes are omitted near the center of the Brillouin zone, the number of contributing modes diverge but the dispersion across the zone remains. This result appears to broaden the scope of validity of the FTG distribution in EVS to non-iid variables. Furthermore, the special scalings that led to the emergence of FTG in the border cases demonstrate new ways of extracting the known limit distribution even in the absence of the conventional FTG scenario.

In summary, the extreme value PDF for Gaussian interface models are, for fixed choice of variables, a two-parameter family of functions with a nonanalytic part for small values, a single maximum, and an essentially exponential tail. The functions look qualitatively similar, but vary quantitatively over the range of parameters d and α studied. This family of curves is different from that found for the roughness distribution for the same parameters α, d [34]. We conclude that it is not possible to make a direct link between non-Gaussian roughness fluctuations and extreme values in these models. Given the multitude of recent observations of non-Gaussian fluctuations in experimental and in model strongly correlated systems, as well as in the use of interface models as phenomenological tools in describing such fluctuations, this seems like an important result. However, the relevance of extreme values in more complex, non-Gaussian systems remains an open question and it would be interesting to follow up this work with studies in this direction.

ACKNOWLEDGMENTS

This work was supported by the Hungarian Academy of Sciences (Grant Nos. OTKA T029792 and T043734) and by CNRS ACI Grant No. 2226. One of us (Z.R.) thanks the Ecole Normale Supérieure for financial support during his visit to Lyon.

APPENDIX A: SMALL-*z* ASYMPTOTE OF THE EXTREME VALUE DISTRIBUTION FOR THE INTENSITIES

1. $d = 1$

Our starting formula is Eq. (9) where, for small z, we expand terms with not too large n to leading order in $n^{\alpha} z$. Terms with larger n's must be considered without expansion. However, exponentiating them the product becomes a sum of logarithms, which we can replace by an integral as the terms vary slowly with n. Carefully treating various corrections allows us to obtain the asymptote for Eq. (9).

Let us separate product (9) for the IPDF, while $z \to 0$, as

$$M_{\alpha}(z) = CD, \tag{A1}$$

where

$$C = \prod_{n=1}^{n_{\alpha}} (1 - e^{-n^{\alpha} z}) \approx \prod_{n=1}^{n_{\alpha}} n^{\alpha} z = z^{n_{\alpha}} (n_{\alpha}!)^{\alpha}, \tag{A2}$$

$$D = \exp\left(\sum_{n=n_{\alpha}+1}^{\infty} \ln[1 - \exp(-n^{\alpha} z)] \right), \tag{A3}$$

with $(n_{\alpha})^{\alpha} z$ small but n_{α} large, i.e.,

$$\frac{1}{z^{1/\alpha}} \gg n_{\alpha} \gg 1. \tag{A4}$$

The first inequality allows the linearization of the exponential in Eq. (A2), whereas the second one will enable us to use the Stirling formula in Eq. (A2) and replace the sum in Eq. (A3) by an integral.

A short detour is necessary to see under what condition the correction to the term linear in z in each factor of Eq. (A2) can be neglected. Including the next term in the expansion we have

$$C \approx \prod_{n=1}^{n_\alpha} n^\alpha z\left(1-\frac{1}{2}n^\alpha z\right) \approx \exp\left(\frac{z}{2}\sum_{n=1}^{n_\alpha} n^\alpha\right)\prod_{n=1}^{n_\alpha} n^\alpha z. \tag{A5}$$

The exponent in the prefactor goes like $z\, n_\alpha^{\alpha+1}$. So the prefactor can be taken as unity if we use an n_α that satisfies

$$\frac{1}{z^{1/(\alpha+1)}} \gg n_\alpha \gg 1, \tag{A6}$$

a condition stricter than Eq. (A4). Then the approximation in Eq. (A2) indeed gives the asymptote of C.

Now we can calculate C from the right hand side of Eq. (A2) by using Stirling's formula

$$C \approx z^{n_\alpha}\left(\frac{n_\alpha}{e}\right)^{\alpha n_\alpha}(2\pi n_\alpha)^{\alpha/2}. \tag{A7}$$

To calculate D we first estimate the error incurred when the sum is written as an integral: given a function $f(z)$, the terms in the sum of $f(n)$ from $n_\alpha+1$ to ∞ can be written to leading order

$$f(n+1) \approx \int_n^{n+1} dx\, f(x) + \frac{1}{2}f'(n+1). \tag{A8}$$

Performing the summation, we can replace the sum of $f'(n+1)$'s by an integral in leading order and we finally find up to the next-to-leading order

$$\sum_{n=n_\alpha}^{\infty} f(n+1) \approx \int_{n_\alpha}^{\infty} dx\, f(x) - \frac{1}{2}f(n_\alpha). \tag{A9}$$

This is the exponent of Eq. (A3) with

$$f(x) = \ln[1-\exp(-x^\alpha z)] \tag{A10}$$

whose integral can be written using $u = xz^{1/\alpha}$ as

$$\begin{aligned}\int_{n_\alpha}^{\infty} dx\, f(x) &= \frac{1}{z^{1/\alpha}}\int_{n_\alpha z^{1/\alpha}}^{\infty} du\, \ln[1-\exp(-u^\alpha)] \\ &\approx \frac{1}{z^{1/\alpha}}\int_0^{\infty} du\, \ln[1-\exp(-u^\alpha)] \\ &\quad - \frac{\alpha}{z^{1/\alpha}}\int_0^{n_\alpha z^{1/\alpha}} du\, \ln u.\end{aligned} \tag{A11}$$

In the last line we used the smallness of u: one can easily convince oneself, from Eq. (A6) that the higher order terms vanish. The definite integral is

$$c(\alpha) = -\int_0^{\infty} du\, \ln[1-\exp(-u^\alpha)] = \zeta\left(1+\frac{1}{\alpha}\right)\Gamma\left(1+\frac{1}{\alpha}\right), \tag{A12}$$

and so from Eq. (A9) we get

$$\ln D \approx -\frac{c(\alpha)}{z^{1/\alpha}} + \alpha n_\alpha - \left(n_\alpha + \frac{1}{2}\right)\ln[(n_\alpha)^\alpha z]. \tag{A13}$$

Finally, Eqs. (A7) and (A13) give

$$M_\alpha(z) \approx \frac{(2\pi)^{\alpha/2}}{\sqrt{z}}\exp\left(-\frac{c(\alpha)}{z^{1/\alpha}}\right). \tag{A14}$$

This is the sought after asymptote for small z in the sense that its relative error vanishes for $z \to 0$.

Remarkably, when we neglect the large n contribution, we find the correct $1/z^{1/\alpha}$ dependence in the argument of the exponential in $M_\alpha(z)$. However, the coefficient $c(\alpha)$ is only found by keeping terms with large n. Note, furthermore, that inequality (A6) needs $\alpha > 0$. Thus we should not be surprised that the asymptote for $\alpha \to 0$ does not relate to the tail of the FTG function (13b) for large negative argument.

In summary, the leading term of $\ln M(z)$ was produced by exponentiating the product and rewriting the sum as an integral. We shall follow this recipe below for general dimensions.

2. Arbitrary dimension

We consider here the asymptotes of IPDF (21). The leading term of the logarithm of the IPDF $M_{\alpha,d}(z)$, in the small-z limit, can be determined by transforming the sum over the modes of the Brillouin zone into an integral, because for $z \to 0$ the terms in the sum change slowly. Thus we obtain, to leading order in z,

$$\ln M_{\alpha,d}(z) \approx -\frac{c(\alpha,d)}{z^{d/\alpha}}, \tag{A15}$$

where

$$\begin{aligned}c(\alpha,d) &= -\frac{1}{2}\int d^d u\, \ln[1-\exp(-|\boldsymbol{u}|^\alpha)] \\ &= \frac{\pi^{d/2}\zeta\left(1+\frac{d}{\alpha}\right)\Gamma\left(1+\frac{d}{\alpha}\right)}{d\Gamma\left(\frac{d}{2}\right)}.\end{aligned} \tag{A16}$$

For $d=1$ we indeed recover $c(\alpha)$ of Eq. (A12). Note that Eq. (A15) does not give the full asymptote for M, it is only the leading term in the exponent.

In order to estimate the next-to-leading term for $\ln M_{\alpha,d}(z)$ one can calculate the correction arising when the sum is transformed into an integral. This is of the order of

$$\frac{\ln z}{z^{(d-1)/\alpha}}. \tag{A17}$$

This correction diverges algebraically for $d>1$, giving rise to a further exponential singularity in the IPDF. The asymptote of M is therefore not as simple as in the 1D case (A14).

APPENDIX B: SMALL-z ASYMPTOTE IN THE CASE OF THE SINE AND COSINE EXPANSION

In this appendix we just summarize the results for the PDF of the maximal square coefficient for the sine and cosine expansion functions. The leading term for the logarithm of IPDF (44) comes from our making the sum an integral

$$\ln \tilde{M}_{\alpha,d}(z) \approx -\frac{\tilde{c}(\alpha,d)}{z^{d/\alpha}}, \tag{B1}$$

where

$$\tilde{c}(\alpha,d) = -\int d^d u \ln[\operatorname{erf}(|\boldsymbol{u}|^{\alpha/2})]. \tag{B2}$$

In $d=1$, after a calculation along a line similar to the one followed in Appendix A, we obtain the full asymptote

$$\tilde{M}_{\alpha,1}(z) \approx \frac{(2\pi)^{\alpha/2}\sqrt{\pi}}{2\sqrt{z}} \exp\left(-\frac{\tilde{c}(\alpha,1)}{z^{1/\alpha}}\right). \tag{B3}$$

Note that the functional form is similar to the asymptote of the IPDF for the maximal intensity (A14), but the constants are different.

APPENDIX C: FINITE-N CORRECTION

Here we calculate the correction of the extreme intensity distribution for large N. Denoting now the finite product (21) by $M_{N,\alpha,d}(z)$ and assuming N to be large we obtain

$$\begin{aligned}\frac{M_{N,\alpha,d}(z)}{M_{\alpha,d}} &= \prod_{|\boldsymbol{n}|>N}{}' \; (1-e^{-|\boldsymbol{n}|^\alpha z}) \\ &\approx 1 - \frac{1}{2}\sum_{|\boldsymbol{n}|>N} e^{-|\boldsymbol{n}|^\alpha z} \\ &= 1 - I_{N,\alpha,d}(z).\end{aligned} \tag{C1}$$

Hence

$$M_{N,\alpha,d}(z) \approx M_{\alpha,d}(z)[1+I_{N,\alpha,d}(z)], \tag{C2}$$

$$P_{N,\alpha,d}(z) \approx P_{\alpha,d}(z) + M_{\alpha,d}(z) I'_{N,\alpha,d}(z), \tag{C3}$$

where the second line was obtained by differentiation and we used the property that I is negligible next to I' for large N. From Eq. (C1) we surmise that the convergence to the $N=\infty$ functions is in essence exponentially fast in N^α; to be specific, we give below for 1D the precise asymptote.

Considering in $d=1$ the $\alpha=1$ case, we have a geometric series as

$$I_{N,1,1}(z) = \sum_{n=N+1}^{\infty} e^{-nz} = e^{-Nz}(e^z-1)^{-1}. \tag{C4}$$

If $\alpha>1$ then

$$\begin{aligned} I_{N,\alpha,1}(z) &= \sum_{n=N+1}^{\infty} e^{-n^\alpha z} = \sum_{n=N+1}^{\infty} e^{-n\, n^{\alpha-1} z} \\ &< \sum_{n=N+1}^{\infty} e^{-n\,(N+1)^{\alpha-1} z} \\ &= \frac{e^{-(N+1)^\alpha z}}{1-e^{-(N+1)^{\alpha-1} z}} \\ &\approx e^{-(N+1)^\alpha z}. \end{aligned} \tag{C5}$$

The last formula, an upper bound for the asymptote, is just the first term in the sum I. The sum has positive terms, whence it follows that the first term is at the same time the asymptote of I for $\alpha>1$. Finally, in the case $\alpha<1$ we can rewrite the sum for I into an integral, because if in Eq. (A8) we substitute $e^{-n^\alpha z}$ for $f(n)$ and $N+1$ for n_α, the correction to the integral is negligible for $\alpha>1$ in the large N limit. The integral is approximately $N^{1-\alpha}e^{-N^\alpha}/\alpha z$, this is then the sought asymptote for I. In conclusion,

$$I_{N,\alpha,1}(z)\begin{cases} \approx e^{-(N+1)^\alpha z} & \text{if } \alpha>1 \\ = e^{-Nz}(e^z-1)^{-1} & \text{if } \alpha=1 \\ \approx N^{1-\alpha}e^{-N^\alpha z}/\alpha z & \text{if } \alpha<1. \end{cases} \tag{C6}$$

We can summarize the above results for various αs such that if the summand in I decays slowly, one can replace the sum by an integral, and if it decays fast then the sum asymptotically equals its first term.

APPENDIX D: ON THE FTG LIMITS

Below we derive Eq. (28) from Eq. (26). We shall replace the lower limit of integration 1 by n_0 to show irrelevance of the precise setting of the lower limit. Denoting the integral in Eq. (26) by I and changing the integration variable to $v=n^\alpha z$ we get

$$I = \frac{1}{\alpha z^{d/\alpha}} \int_{n_0^\alpha z}^{\infty} e^{-v} v^{d/\alpha-1} dv. \tag{D1}$$

Since $\alpha\to 0$, the lower integration limit becomes z, indeed independent of n_0. The saddle point method gives

$$I \approx \sqrt{\frac{\pi}{2\alpha d}} \left(\frac{d}{z\alpha e}\right)^{d/\alpha} \operatorname{erfc}\left(\frac{z\alpha - d}{\sqrt{\alpha d}}\right). \tag{D2}$$

When $z\approx d/\alpha e$, the argument of the erfc becomes a large negative number, where the erfc is approximately 2. Thus, including the prefactor before I in Eq. (26), we recover Eq. (28).

We have here an opportunity to test whether the sum in Eq. (26) was justly rewritten into an integral. We do not have rigorous results, but we know that the integral must not be smaller than a single summand term, if it is, the integral representation cannot be accepted. A characteristic summand term now is $e^{-n^{\alpha}z}\approx e^{-v}$, where $v=(d-1)/\alpha$ is the saddle point in Eq. (D1), so the summand term is small. Since we consider z's for which the full integral for $-\ln M$ is $O(1)$, the integral is indeed much larger than a single characteristic summand term e^{-v}. This is a generic test that the integral representation of a sum should pass, and we performed it in all pertinent cases in the paper.

APPENDIX E: SMALL-*z* ASYMPTOTE OF THE ROUGHNESS DISTRIBUTION

1. One dimension, $\alpha>1$

We derive here the small-x asymptote of the PDF of the roughness for the Gaussian model of $1/f^{\alpha}$ noise with periodic boundary condition. We consider the case $\alpha>1$, when all cumulants of the roughness are of the same order. In the case of the Wiener process, $\alpha=2$, the PDF has a nonanalytic asymptote, which has been calculated in Ref. [31]. Here we find that nonanalyticity prevails for all $\alpha>1$. We begin with the simplest form, free of normalizing constants, of the generating function [34]

$$G_{\alpha}(s)=\prod_{n=1}^{\infty}\left(1+\frac{s}{n^{\alpha}}\right)^{-1}. \tag{E1}$$

The average is given by $-G_{\alpha}'(0)=\zeta(\alpha)$, where ζ is Riemann's zeta function, so in order to obtain a PDF normalized to unit average, in the end we should rescale by $\zeta(\alpha)$.

The large-s asymptote of the generating function will give us the initial asymptote of the PDF. The calculation goes along the lines of Appendix A. For large s we can factorize G_{α} as

$$G_{\alpha}(s)=EF, \tag{E2}$$

where

$$E=\prod_{n=1}^{n_{\alpha}}\left(1+\frac{s}{n^{\alpha}}\right)^{-1}\approx\prod_{n=1}^{n_{\alpha}}\frac{n^{\alpha}}{s}=s^{-n_{\alpha}}(n_{\alpha}!)^{\alpha}, \tag{E3}$$

$$F=\exp\left[-\sum_{n=n_{\alpha}+1}^{\infty}\ln\left(1+\frac{s}{n^{\alpha}}\right)\right], \tag{E4}$$

where

$$s^{1/(\alpha+1)}\gg n_{\alpha}\gg 1. \tag{E5}$$

The first inequality ensures that Eq. (E3) indeed gives the asymptote for E, see Appendix A for an analogous estimate, and the largeness of n_{α} enables us to approximate the sum in Eq. (E4) by an integral. We also calculate in F the nonvanishing corrections to the integral, again in a way similar to what was done in Appendix A. Then using the Stirling formula in Eq. (E3) for E, substituting E and F into Eq. (E2), and collecting all stray terms we wind up for large s with

$$G_{\alpha}(s)\approx(2\pi)^{\alpha/2}\sqrt{s}\exp[-s^{1/\alpha}g(\alpha)], \tag{E6}$$

where

$$g(\alpha)=\int_0^{\infty}du\,\ln(1+u^{-\alpha})=\frac{\pi}{\sin\left(\frac{\pi}{\alpha}\right)}. \tag{E7}$$

The PDF of the roughness, normalized to unit mean, is obtained by inverse Laplace transformation

$$P_{\alpha}(x)=\int\frac{ds}{2\pi i}e^{sx}G_{\alpha}\left(\frac{s}{\zeta(\alpha)}\right). \tag{E8}$$

For small x the large-real-s region dominates, where the saddle point method can be used. It suffices to compute the saddle point from the exponential of Eq. (E6), and then substitute its value into the $\sqrt{s}$ prefactor. Taking into account also the quadratic deviation from the saddle point in the exponent, we finally obtain the small-x asymptote

$$P_{\alpha}(x)\approx Q(\alpha)x^{-(3\alpha-1)/2(\alpha-1)}\exp\left(-\frac{R(\alpha)}{x^{1/(\alpha-1)}}\right), \tag{E9}$$

where

$$Q(\alpha)=\frac{(2\pi)^{(\alpha-1)/2}g(\alpha)^{\alpha(\alpha-1)}}{\sqrt{\alpha-1}[\alpha\zeta(\alpha)]^{(\alpha+1)/2(\alpha-1)}}, \tag{E10}$$

$$R(\alpha)=\frac{(\alpha-1)\,g(\alpha)^{\alpha(\alpha-1)}}{\alpha^{\alpha/(\alpha-1)}\,\zeta(\alpha)^{1/(\alpha-1)}}. \tag{E11}$$

2. Arbitrary dimension, $\alpha>d$

In general dimensions we can give here only the leading exponential for the initial asymptote of the PDF of the roughness for periodic boundary condition. We consider the case $\alpha>d$, else there is no sense in speaking about the asymptote for small roughness on the scale $L^{d-\alpha}$, see Ref. [34]. The generating function yielding unit average is from Ref. [34]

$$G_{\alpha,d}(s)=\prod_{|\boldsymbol{n}|>0}\left(1+\frac{s}{\zeta(\alpha,d)|\boldsymbol{n}|^{\alpha}}\right)^{-1/2}, \tag{E12}$$

where

$$\zeta(\alpha,d)=\frac{1}{2}\sum_{|\boldsymbol{n}|>0}|\boldsymbol{n}|^{-\alpha} \tag{E13}$$

is a d-dimensional generalization of the zeta function. Exponentiation of the product to a sum and transformation of the sum to an integral gives the leading exponential term

$$\ln G_{\alpha,d}(s) \approx -\left(\frac{s}{\zeta(\alpha,d)}\right)^{d/\alpha} g(\alpha,d), \tag{E14}$$

where

$$g(\alpha,d) = \int_0^\infty d^d u \ln(1+|\boldsymbol{u}|^{-\alpha}) = \frac{\pi^{d/2+1}}{d\Gamma\left(\frac{d}{2}\right)\sin\left(\frac{\pi d}{\alpha}\right)}. \tag{E15}$$

Performing the inverse Laplace transformation by the saddle point method, one arrives at the small-x asymptote of the PDF as

$$\ln P_{\alpha,d}(x) \approx -\frac{R(\alpha,d)}{x^{d/(\alpha-d)}}, \tag{E16}$$

with

$$R(\alpha,d) = \frac{\alpha-d}{d}\left[\frac{\pi^{d/2+1}}{\alpha\Gamma\left(\frac{d}{2}\right)\sin\left(\frac{\pi d}{\alpha}\right)\zeta(\alpha,d)^{d/\alpha}}\right]^{\alpha/(\alpha-d)}. \tag{E17}$$

[1] S. Coles, *An Introduction to Statistical Modeling of Extreme Values*, Springer Series in Statistics (Springer-Verlag, London, 2001).
[2] J.-P. Bouchaud and M. Mézard, J. Phys. A **30**, 7997 (1997).
[3] S.N. Majumdar and P.L. Krapivsky, Physica A **318**, 161 (2003).
[4] A. Baldassarri, A. Gabrielli, and B. Sapoval, e-print cond-mat/0205130.
[5] K. Dahlstedt and H.J. Jensen, J. Phys. A **34**, 11 193 (2001).
[6] R. Skoe, D. Vandembroucq, and S. Roux, Int. J. Mod. Phys. C **13**, 751 (2002).
[7] G. D'Anna, P. Mayor, G. Gremaud, A. Barrat, and V. Loreto, Europhys. Lett. **61**, 60 (2003).
[8] J. Galambos, *The Asymptotic Theory of Extreme Order Statistics* (Krieger, Malabar, Florida, 1987).
[9] In the statistical physics literature the limit functions are often called universal, but we do not use this term here in order to avoid confusion with universality in critical systems.
[10] D.S. Dean and S.N. Majumdar, Phys. Rev. E **64**, 046121 (2001).
[11] M. Praehofer and H. Spohn, J. Stat. Phys. **108**, 1071 (2002).
[12] Z. Toroczkai, G. Korniss, S. Das Sarma, and R.K.P. Zia, Phys. Rev. E **62**, 276 (2000).
[13] P.-M. Lam and S. Tan, Phys. Rev. E **62**, 6246 (2000).
[14] Z. Toroczkai and G. Korniss, Phys. Rev. E **64**, 048101 (2001).
[15] S. Raychaudhuri, M. Cranston, C. Przybyla, and Y. Shapir, Phys. Rev. Lett. **87**, 136101 (2001).
[16] S.T. Bramwell, P.C.W. Holdsworth, and J.-F. Pinton, Nature (London) **396**, 552 (1998).
[17] S.T. Bramwell, J.-Y. Fortin, P.C.W. Holdsworth, S. Peysson, J.-F. Pinton, B. Portelli, and M. Sellitto, Phys. Rev. E **63**, 041106 (2001).
[18] S.C. Chapman, G. Rowlands, and N.W. Watkins, Nonlinear Proc. Geoph. **9**, 409 (2003).
[19] N.W. Watkins, S.C. Chapman, and G. Rowlands, Phys. Rev. Lett. **89**, 208901 (2002).
[20] S.T. Bramwell *et al.*, Phys. Rev. Lett. **89**, 208902 (2002).
[21] T. Antal, M. Droz, G. Györgyi, and Z. Rácz, Phys. Rev. Lett. **87**, 240601 (2001).
[22] R. Labbé, J.-F. Pinton, and S. Fauve, J. Phys. II **6**, 1099 (1996).
[23] J.-F. Pinton, P.C.W. Holdsworth, and R. Labbé, Phys. Rev. E **60**, R2452 (1999).
[24] D. Lathrop, J. Fineberg, and H. Swinney, Phys. Rev. A **46**, 6390 (1992).
[25] B.A. Carreras *et al.*, Phys. Rev. Lett. **83**, 3653 (1999).
[26] S.T. Bramwell *et al.*, Phys. Rev. Lett. **84**, 3744 (2000).
[27] S. Aumaître, S. Fauve, S. McNamara, and P. Poggi, Eur. Phys. J. B **19**, 449 (2001).
[28] A. Noullez and J. Pinton, Eur. Phys. J. B **28**, 231 (2002).
[29] I. Janosi and J. Gallas, Physica A **271**, 448 (1999).
[30] S. Bramwell, T. Fennell, P. Holdsworth, and B. Portelli, Europhys. Lett. **57**, 310 (2002).
[31] G. Foltin, K. Oerding, Z. Rácz, R.L. Workman, and R.K.P. Zia, Phys. Rev. E **50**, R639 (1994).
[32] Z. Rácz and M. Plischke, Phys. Rev. E **50**, 3530 (1994).
[33] M. Plischke, Z. Rácz, and R.K.P. Zia, Phys. Rev. E **50**, 3589 (1994).
[34] T. Antal, M. Droz, G. Györgyi, and Z. Rácz, Phys. Rev. E **65**, 046140 (2002).
[35] B. Portelli and P. Holdsworth, J. Phys. A **35**, 1231 (2002).
[36] T.M. Apostol, *Modular Functions and the Dirichlet Series in Number Theory* (Springer-Verlag, New York, 1976).
[37] The FTG IPDF is often written as $M_{\rm FTG}(y)=e^{-e^{-y}}$. The present form (13a), however, has a natural scale for the extremal variable. Namely, in order to test whether an empirical extremal quantity z is of the FTG class, one can compute the variable $y=(z-\langle z\rangle)/\Delta z$, where $\langle z\rangle$ and Δz are the mean and the standard deviation of z, respectively, and compare the distribution of y to Eq. (13).
[38] Traditionally, the term parent PDF refers to the single distribution function of iid variables, but we shall speak about parent PDFs also in the case, when the variables are independent, but differently distributed.